Rheology, Morphology, Mechanical Properties and Free Volume of Poly(trimethylene terephthalate)/Polycarbonate Blends

Indose Aravind,[†] Kyung Hyun Ahn,[‡] C. Ranganathaiah,[§] and Sabu Thomas*[,†]

School of Chemical Sciences, Mahatma Gandhi University, Priyadarshini Hills P.O., Kottayam, 686 560, India, School of Chemical and Biological Engineering, Seoul National University, Seoul, 151-744, Korea, and Department of Studies in Physics, University of Mysore, Manasagangotri, Mysore, 570 006, India

The phase morphology, rheology, mechanical properties, and free volume of poly(trimethylene terephthalate)/polycarbonate (PTT/PC) blends have been investigated as a function of composition. The morphology indicated a two-phase structure, and the blends showed co continuous phase morphology between 30−60 wt % of poly carbonate. Due to the high viscosity of PC, PTT is more finely dispersed in the PC matrix than PC in the PTT matrix. The rheological measurements of the blends revealed that the complex viscosity increased with increase in PC content. Relatively low interfacial tension values of the blends determined using Palierne and Choi−Schowalter methods indicated that there is considerable interaction between the blend components (PTT and PC) due to the transesterification reactions. A random copolyester formed as a result of the transesterification acted as a compatibilizer in the initial stages of reactions which is the main factor for the change in miscibility. The phase morphology and the interfacial adhesion influence the mechanical properties such that addition of the PC phase decreases the tensile strength and Young's modulus of the system. The free volume data from PALS results showed a slight positive deviation from the known linear additivity rule with increase in PC content, suggesting the blends are partially miscible. Our results show a good correlation among the phase morphology, rheology, mechanical, and free volume parameters.

1. Introduction

High performance polymeric materials suitable to industrial needs can be obtained by simple blending of polymers. An adequate polymer blend process requires information on the blend flow behavior under production process conditions. However, most polymer pairs are intrinsically immiscible giving rise to lower mechanical properties. Blend morphology is affected by rheological characteristics of the base polymers, and shear stress applied during the mixing of the components.[1−3] In order to design proper molds, make appropriate process equipment selection, and assess of the optimum process conditions, it is very important to know the relationship among the melt viscosity, elasticity, shear rate, pressure, and processing temperature. Rheology is one of the most frequently used methods for characterizing interfacial properties such as interfacial tension and strength that are necessary for predicting the mechanical properties of immiscible polymer blends.[4,5] The rheological properties of molten components in immiscible polymer blends affect the processing/morphology/property relationships.[6−10] The classic theory of rheology of emulsions focuses on dilute emulsions of spherical, Newtonian drops.[11,12] Palierne[13] reported a cell theory for more concentrated emulsions that applies to dynamic shear with very small drop deformation from a spherical shape. Computational results on concentrated emulsion rheology were repoted by Loewenberg and Hinch[14] for shear flows with appreciable departures from a spherical shape for the dispersed phase. The Palierne theory has an added distinction of being formulated for viscoelastic constituents. The Oldroyd[15] and Choi and Schowalter[16] models are the other two models of emulsion rheology that are applied widely to polymer blends in the dilute and semidilute regimes to explain their rheological behavior.

The phase morphology and rheology of multiphase polymer blends are strongly affected by interfacial characteristics. Asthana and Jayaraman[17] and Shi et al.[18] reported that the interfacial tension in polymer blends can be estimated from particle size distribution using the Palierne model. Also, Friedrich et al.[19] have shown that if the interfacial tension is known, the particle size distribution can be derived from measured data. Micromechanical models, such as that of Coran and Patel,[20] reflect the morphology, together with the common series and parallel mixing rule approaches, and have been used to describe the observed rheological response.[21]

Sorona (the trade name for a new generation biobased polymer from DuPont) is basically poly(trimethylene terephthalate) made by the condensation polymerization of corn-derived 1,3-propanediol and terephthalic acid. The new polymer, Sorona, has exceptional properties like softness, stretch with recovery, resilience, stain resistance, easy dyeability for fibers, and high air impermeability. Polycarbonate has several advantages like thermal stability, toughness, transparency, etc. Sorona/polycarbonate (PC) blends are of commercial interest because of their potential combination of impact strength, modulus, and heat, chemical, and abrasion resistance. The important studies of PTT blends include PTT/PA12,[3] PTT/ethylene propylene diene monomer (EPDM),[22−24] PTT/PC,[25−29] PTT/polypropene (PP),[30] and PTT/poly(hexamethylene isophthalamide) blends.[31]

In the present study, the phase morphology, rheological, mechanical, and free volume parameters of Sorona/polycarbonate blends were analyzed. When the PTT/PC blends were thermally annealed at high temperatures, various extents of transreactions occur between the two polymers. Under the reaction conditions of rheology measurements, some amount of transreactions occur between the blend components which is evidenced by calculating interfacial tension values. Dynamic

* To whom correspondence should be addressed. E-mail: sabut552001@yahoo.com. Tel.: 0091-481-2730003. Fax: 0091-481-2731002.
[†] Mahatma Gandhi University.
[‡] Seoul National University.
[§] University of Mysore.

10.1021/ie9007503 CCC: $40.75
Published on Web 07/31/2009

rheological measurements using a plate/plate rheometer have been employed to evaluate the viscoelastic properties such as complex viscosity, storage modulus, etc. Phase morphology analysis was done using SEM. Mechanical properties were measured using Universal testing machine. Free volume measurements were done using a Positron Lifetime spectrometer. Further, an attempt has been made to correlate phase morphology with rheological, mechanical, and free volume parameters. Finally, the experimental results were compared with results from different theoretical models.

2. Experimental Section

2.1. Materials. Sorona (PTT) in pellet form was supplied by DuPont, USA. The PC used was a product from LG Dow Chemical Co. with a melt flow rate of 30 g/10 min (ASTM D1238, 300 °C/1.2 kg). Blends were prepared in a Haake mixer at 260 °C for 5 min with a rotor speed of 60 rpm. Before melt mixing, PTT and PC were dried under vacuum at 105 °C for at least 16 h to minimize the possibility of hydrolysis during the mixing.

2.2. Blend Preparation. Blends of different compositions of PTT and PC (PTT_{90} to PTT_{10}, where PTT denotes Sorona and subscript denotes the percentage composition by weight of PTT) were prepared by melt mixing of PTT with PC in a Haake mixer at 260 °C with a rotor speed of 60 rpm, and mixing time was optimized at 5 min. The melt mixed samples were then compression molded at 260 °C to obtain sheets of 1 mm thickness.

2.3. Phase Morphology Measurements. The morphology of the blends was analyzed using a Jeol scanning electron microscope (SEM; Jeol 5400, Tokyo, Japan). The samples for the morphology measurements were prepared by cryogenically fracturing the samples in liquid nitrogen. The dispersed PC phase is preferentially extracted from the blend using methylene chloride. The size of the dispersed phase was analyzed by an image analysis technique. About 300 particles were considered for the diameter measurements. The number average (D_n) and weight average diameters (D_w), polydispersity index (pdi), and interfacial area per unit volume (A_i) were determined using the following equations:

The number average diameter

$$D_n = \frac{\sum N_i D_i}{\sum N_i} \tag{1}$$

The weight average diameter

$$D_w = \frac{\sum N_i D_i^2}{\sum N_i D_i} \tag{2}$$

Polydispersity index

$$\text{pdi} = \frac{D_w}{D_n} \tag{3}$$

Interfacial area per unit volume

$$A_i = \frac{3\phi}{\mathbf{R}} \tag{4}$$

Interparticle distance

$$\text{IPD} = D\left[\left(\frac{\pi}{6\phi}\right)^{1/3} - 1\right] \tag{5}$$

where ϕ is the volume fraction and **R** the average radius of the dispersed particles.

2.4. Dynamic Rheology. The rheological properties of the blends were evaluated on a Rheometric Scientific ARES (TA Instruments) rheometer in plate/plate geometry. Disc-shaped samples of 25 mm diameter and 1 mm thickness were prepared using metal plates of suitable dimension by compression molding technique. The samples were placed between the hot plates which are kept at 260 °C for 5 min. A temperature/frequency sweep method was selected and the frequency range was taken as 0.1 to 100 rad/s at 260 °C under vacuum. The strain was taken as 10%. From the rheological measurements, the shear modulus (G') and complex viscosity (η^*) etc. have been obtained.

2.5. Tensile Properties. The static tensile experiments were performed on the MTS Synergie RT1000 testing apparatus. The loading speed was 1 mm/min. Extensometer HTE was used with a nominal length of 10 mm. Tensile specimens were punched out from the compression-molded films. Tensile testing of dumbbell-shaped specimens was carried out at cross head speeds of 10 mm/min and a gauge length of 3 cm.

2.6. Positron Annihilation Lifetime Spectroscopy (PALS) Measurements. The PALS spectrometer consisted of a fast−fast coincidence system with BaF_2 Scintillators coupled to XP2020/Q photomultiplier tubes with quartz windows as detectors. The detectors were cone-shaped to achieve better time resolution. A 17 μCi 22Na positron source, deposited on a pure Kapton foil of thickness 0.0127 mm was placed between the two identical pieces of the sample under investigation. This sample−source sandwich was positioned between the two detectors of the system to acquire the lifetime spectrum. The spectrometer measures 180 ps as the resolution function with a ^{60}Co source. However, for better count rates, the spectrometer was operated at 220 ps resolution. All lifetime measurements were performed at room temperature and two or three positron lifetime spectra (with more than a million counts in each spectrum) were recorded. The consistently reproducible spectra were analyzed into three lifetime components with the help of the PATFIT-88[32] computer program with proper source and background corrections. The source correction term and resolution function were estimated from the lifetime of well-annealed aluminum using the RESOLUTION[32] program. The three Gaussian resolution functions were used in this analysis of positron lifetime spectra for the blend and pure samples.

3. Results and Discussion

3.1. Phase Morphology and Rheology Analysis. It should be noted that the viscosity difference between polymers has a significant impact on the phase morphology of the blends. If the minor component has lower viscosity compared to the major one, it will be finely and uniformly dispersed in the major continuous phase owing to the diffusional restrictions imposed by the matrix[3] and otherwise coarsely dispersed. It is believed that the viscosity ratio should be approximately unity when designing the polymer blends for superior properties. Wu's equation (eq 6) suggests that minimum particle size is achieved when the viscosities of the two phases are closely matched, and as the viscosity moves away from unity in either direction, the dispersed particles become larger.[33]

$$D = \frac{4\Gamma\lambda^{\pm 0.84}}{\dot{\gamma}\eta_m} \quad (6)$$

where D is the droplet diameter, η_m, the viscosity of the matrix, λ, the viscosity ratio of the droplet phase to the matrix, $\dot{\gamma}$, the shear rate, and Γ, the interfacial tension.

We observed a similar result from the SEM micrographs of PTT/PC blends presented in Figure 1. The SEM pictures reveal that from 10 to 30 wt % of polycarbonate in the blend, the PTT phase is the matrix and PC is the dispersed phase. The variation in dispersed particle size (D_n and D_w) with PC content is presented in Figure 2. It is obvious from this that as the weight percent of PC in the PTT matrix increases particle size increases and beyond a certain limit of composition (30 wt %) both PTT and PC form a cocontinuous phase structure. The phase inversion occurs at PTT/PC, 40/60 composition where PC forms the matrix in which PTT is distributed as dispersed particles. This is a typical morphology of an incompatible heterogeneous binary blend. It should be noted that the less viscous component (PTT) forms smaller dispersed particles in a more viscous matrix (PC) due to the comparatively restricted diffusion effects on coalescence of particles and increased shear stress resulting from the more viscous matrix phase. This is evident from the polydispersity index values shown in Figure 3. Further, it can be observed that when the concentration of dispersed phase increases, due to the enhanced unfavorable cross-correlations of the component polymers at the interface between them (derived from the surface tensional forces), the morphology becomes more coarse and unstable. It is noteworthy that blends with a dispersed PTT phase possess more uniform morphology compared to those with a dispersed PC phase. This behavior is due to the fact that the relatively more viscous PC matrix facilitates the formation of more uniform dispersed morphology. The effect of blend ratio on the domain distribution of the dispersed phase in PTT/PC blends is shown in Figure 4. It can be seen that when the dispersed phase concentration is low, the domain distribution become narrower compared to a higher dispersed phase concentration; i.e., the blends containing 10 wt % PC (PTT_{90}) and 20 wt % PTT (PTT_{20}) show the narrowest distributions while PTT_{70} and PTT_{40} show the broadest distributions of particles. The distribution of domains in all the other blends remains in between these two limits. This is expected and can be directly related to the relative stability of phase structure. Figure 5 displays the effect of blend ratio on the interfacial area per unit volume (A_i) and interparticle distance (IPD) of PTT/PC uncompatibilized blends. It is evident from the figure that A_i diminishes with increasing concentration the minor component in the blend. Blends with a dispersed PTT phase possess greater interfacial area compared to the corresponding blends with a PC dispersed phase. This is because A_i depends on the average domain size of dispersed particles. On the other hand, on the basis of A_i values, one can claim that blends with lower A_i exhibit maximum unfavorable interactions (derived from maximum interfacial tension) at the interface and are thus associated with more coarse, nonuniform, and unstable morphology. The higher value of IPD indicates the tendency of a material to be failed brittley upon mechanical loading. It is obvious from the figure that with increasing concentration of PTT dispersed phase in the blend, IPD increases in all blends except for PTT_{40}, suggesting that the blends are prone for brittle failure with increasing concentration of PTT in the PC component. In short, the morphological parameters showed that all blends are associated with two-phase morphology owing to greater coalescence effects in the absence of favorable interactions at the interface between the phases. As the concentration

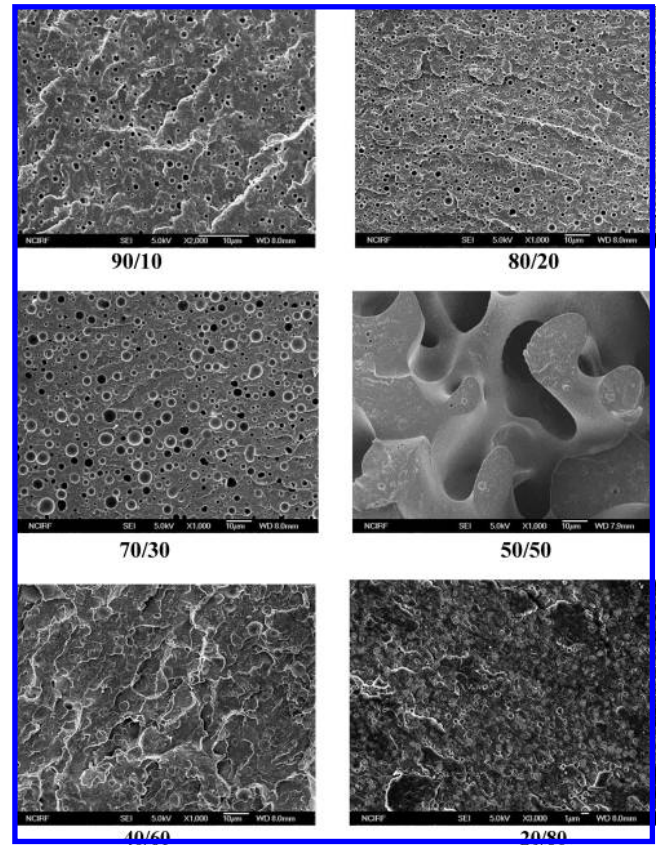

Figure 1. Scanning electron micrographs of PTT/PC blends.

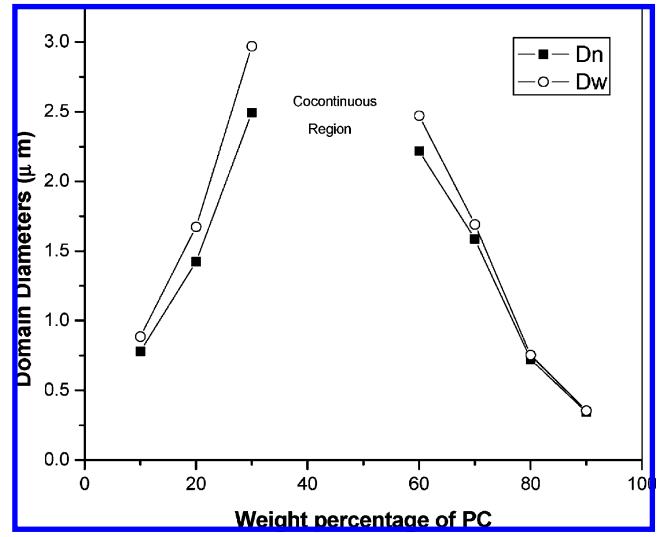

Figure 2. Effect of PC concentration on D_n and D_w of PTT/PC blends.

of one phase in the blends increases, the incompatibility intensifies. It should be noted that the melt blended samples were directly used for SEM analysis, and therefore, there is not any possibility of transesterification reactions to take place to improve the miscibility between the blend components.

But under the reaction conditions of melt rheological measurements (5 min compression molding for making samples, 2 min annealing time before rheological measurements, and 20 min for melt rheological analysis), there is sufficient time for the transesterification reaction to occur between the blend components. From the literature, it can be seen that solution-cast PTT/PC blends are inherently immiscible,[34] and after annealing at 260 °C, the blends could become miscible due to

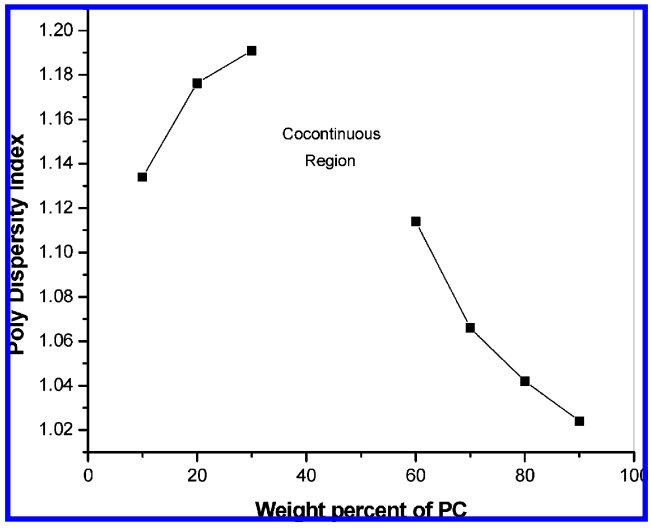

Figure 3. Variation of polydispersity index with PC concentration.

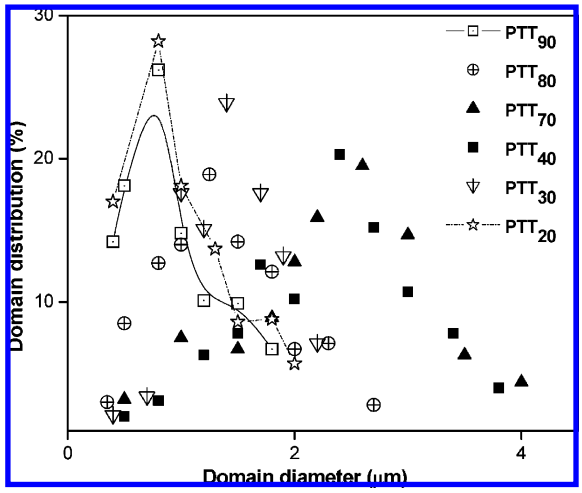

Figure 4. Effect of blend ratio on the domain distribution of PTT/PC blends (trend lines for PTT_{90} and PTT_{20} are given only in order to distinguish narrow distributions).

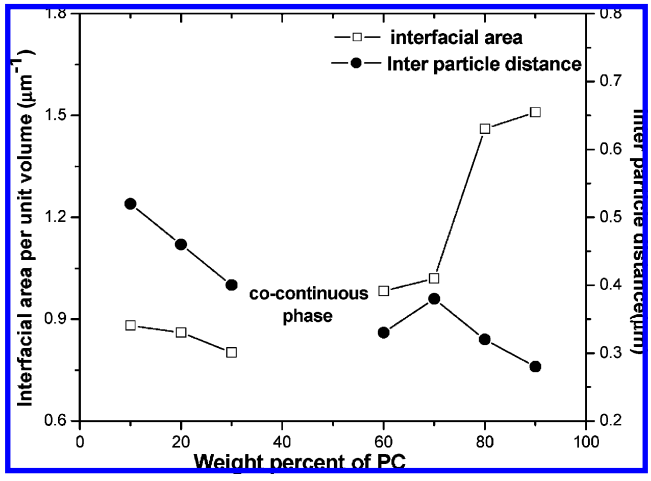

Figure 5. Effect of blend ratio on the interfacial area per unit volume and interparticle distance of PTT/PC blends.

the transesterification reaction. According to Yavari et al.,[28] PTT/PC blends are partially miscible and after annealing at 300 °C for 10 min the blends changed to a miscible state through a transesterification reaction. From these investigations, it can be concluded that transesterification plays an important role in controlling the properties of PTT/PC blends.

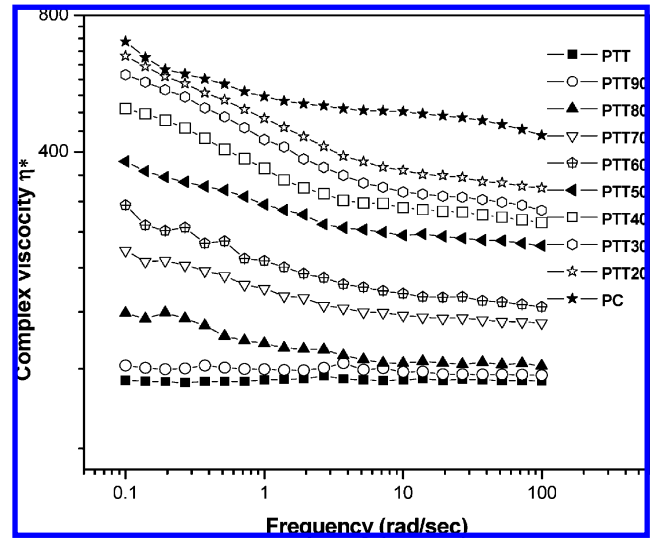

Figure 6. Effect of blend ratio on the complex viscosity of PTT/PC blends.

Effect of blend ratio on the complex viscosity of uncompatibilised PTT/PC blends is given in Figure 6. As the frequency increases, the complex viscosity decreases. Further, with increase in frequency, the relaxation time decreases, or in other words, the shear rate increases. Thus an increase in frequency has the same effect as that of increase in shear rate. Thus in all cases, pseudoplastic behavior is seen. It is seen from the Figure 6 that PTT has the minimum while PC has the maximum complex viscosity in the whole range of frequency. The complex viscosity of all the blends is found to be intermediate between the neat polymers in such a way that addition of PC into PTT increases the complex viscosity due to the interaction between blend components because of trans reaction took place between the components.

3.1.1. Theoretical Modeling of Rheological Properties. In polymer blends, in addition to the characteristics of the component polymers, the viscosity depends on the interfacial adhesion. This is because, in polymer blends, there is interlayer slip along with the orientation and disentanglement upon the application of shear stress. When shear stress is applied to a blend, it undergoes an elongational flow. If the interface is strong, the deformation of the dispersed phase is effectively transferred to the continuous phase. However, in the case of a weak interface, interlayer slip occurs and, as a result, the viscosity of the system decreases. In order to compare the rheological behavior of binary blends, the theoretically predicted viscosities of the uncompatibilized PTT/PC blends for the entire composition range were calculated using different rheological models (eqs 7−10).

The viscosity of a biphasic system can be calculated using a series of mixing rules.

According to the rule of additivity[35]

$$\eta = \eta_1\phi_1 + \eta_2\phi_2 \tag{7}$$

For heterogeneous materials, Hashin's upper and lower limit models[36] suggest that

$$\eta_{mix} = \eta_2 + \frac{\phi_1}{\frac{1}{(\eta_1 - \eta_2)} + \frac{\phi_2}{2\eta_2}} \tag{8}$$

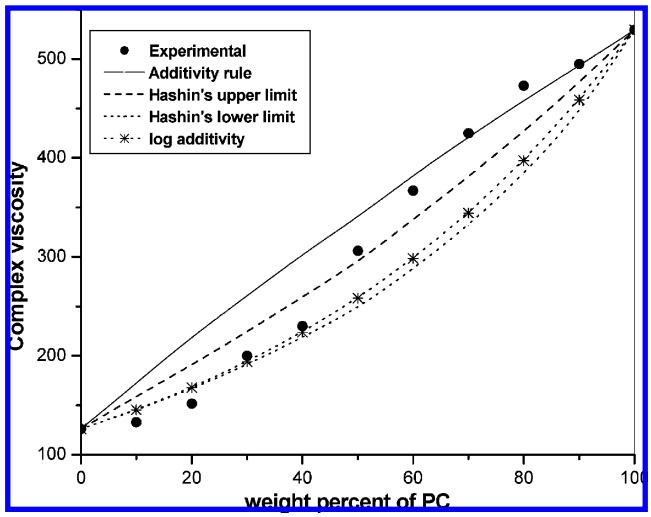

Figure 7. Theoretical modeling of the complex viscosity of PTT/PC blends at a frequency of 1 Hz.

$$\eta_{mix} = \eta_1 + \frac{\phi_2}{\frac{1}{(\eta_2 - \eta_1)} + \frac{\phi_1}{2\eta_1}} \tag{9}$$

where, η_{mix} is the viscosity of the blend, η_1, η_2, and ϕ_1, ϕ_2 are the viscosities and volume fractions of the pure components, respectively.

The log additivity rule assumes that the viscosity of the blend depends on their logarithmic addition[35]

$$\log \eta_{mix} = \sum c_i \log \eta_i \tag{10}$$

where, c_i is the weight fraction and η_i is the viscosity of the components.

Figure 7 presents the comparison of the experimental value of complex viscosities of the uncompatibilized blends with those predicted by the theoretical rheological models at a frequency of 1 Hz. It can be seen from Figure 7 that the blends exhibit a positive−negative deviation behavior from the additivity line. Similar behavior was also reported earlier by Utracki[1,35] for polybutadiene−polyisoprene blends. Here when the PC content in the blend is increased from 10−60 wt %, the experimental viscosity of the blends show a negative deviation from additivity line model values. But above 60 wt % PC content, the viscosity of the blends follows a slight positive deviation from the additivity line. When PC is the dispersed phase in the PTT matrix, the experimental values seem to lie close to those of Hashin's lower limit and log additivity values show a positive deviation from 50 wt % PC more toward the values as predicted by the additivity rule. An immiscible blend can exhibit three types of behavior: (a) positive deviation as in a homogeneous blend in which there is a large interaction between the phases; (b) negative deviation when the interaction is small; and (c) a positive−negative deviation, when there is a concentration-dependent change of structure. Therefore the positive−negative deviation observed for the PTT/PC system is expected to be the result of change in the phase morphology and interfacial interactions due the transesterification reactions that occurred.

3.1.2. Interfacial Tension Measurements. The Palierne model has been shown to be very useful for predicting the rheological behavior of the immiscible blends which describes the linear viscoelastic behavior of emulsions of viscoelastic fluids.[37−40] Also, the Palierne model was used to determine the interfacial tension between the components[37,41] to determine the volume average radius of the dispersed particles,[42] to calculate the sphere-size distribution from rheological data[43] and to analyze the deformation of droplets under elongational flow.[44] With an electric formalism, Palierne derived an equation for predicting the complex modulus of molten (emulsion type) blends (G^*_b), which is a function of the complex moduli of both phases G^*_m (for the matrix) and G^*_b (for the inclusions or dispersed phase) taking into account of several important features of a multiphase system. The viscoelasticity of phases, the hydrodynamics interactions, the droplet size and size distribution, and the interfacial tension are indeed included in this formulation.

Jacobs et al.[45] developed an extended form of the Palierne model, written as

$$G^*_b = G^*_m \frac{1 + 3\int_0^\infty \frac{E(\omega,R)}{D(\omega,R)}\nu(R)\,dR}{1 - 2\int_0^\infty \frac{E(\omega,R)}{D(\omega,R)}\nu(R)\,dR} \tag{11}$$

in which

$$E(\omega,R) = \left([G^*_d(\omega) - G^*_m(\omega)][19G^*_d(\omega) + 16G^*_m(\omega)] + \frac{4\alpha}{R}\right)[5G^*_d(\omega) - 2G^*_m(\omega)] + \frac{\beta^{I}(\omega)}{R}[23G^*_d(\omega) - 16G^*_m(\omega)] + \frac{2\beta^{II}(\omega)}{R}[13G^*_d(\omega) - 8G^*_m(\omega)] + \frac{24\beta^{II}(\omega)\alpha}{R^2} + 16\beta^{II}(\omega)\frac{\alpha + \beta^{I}(\omega)}{R^2} \tag{12}$$

and

$$D(\omega,R) = [2G^*_d(\omega) + 3G^*_m(\omega)][19G^*_d(\omega) + 16G^*_m(\omega)] + \frac{40\alpha}{R}[G^*_d(\omega) + G^*_m(\omega)] + \frac{2\beta^{I}(\omega)}{R}[23G^*_d(\omega) + 32G^*_m(\omega)] + \frac{4\beta^{II}(\omega)}{R}[13G^*_d(\omega) + 12G^*_m(\omega)] + \frac{48\beta^{I}(\omega)\alpha}{R^2} + 32\beta^{II}(\omega)\frac{\alpha + \beta^{I}(\omega)}{R^2} \tag{13}$$

where, $G^*_b(\omega)$, $G^*_m(\omega)$, and $G^*_d(\omega)$ represent complex modulus of blend, matrix, and dispersed phase, respectively. $\beta^{I}(\omega)$ and $\beta^{II}(\omega)$ are the complex interfacial dilation and shear moduli, respectively. $\nu(R)$ denotes the particle size distribution function while R, α, and ω are particle radius, interfacial tension, and strain frequency, respectively. When the deformation of the dispersed phase is small enough so that viscoelastic properties remain linear, we can set both $\beta^{I}(\omega)$ and $\beta^{II}(\omega)$ to zero. Graebling et al.[37] by assuming the particle size distribution to be narrow ($R_v/R_n \leq 2$) and interfacial tension to be independent of shear and interfacial area variation simplified the equation as follows:

$$G^*_b = G^*_m \frac{1 + 3\sum_i \varphi_i H_i(\omega)}{1 - 2\sum_i \varphi_i H_i(\omega)} \tag{14}$$

where

$$H_i(\omega) = \frac{(4\alpha/R_i)(2G^*_m(\omega) + 5G^*_d(\omega)) + (G^*_d(\omega) - G^*_m(\omega))(16G^*_m(\omega) + 19G^*_d(\omega))}{(40\alpha/R_i)(G^*_m(\omega) + G^*_d(\omega)) + (2G^*_d(\omega) - 3G^*_m(\omega))(16G^*_m(\omega) + 19G^*_d(\omega))} \tag{15}$$

Table 1. Interfacial Tension Values of PTT/PC Blends

blend	interfacial tension (mN/m)	
	Palierne	Choi−Schowalter
PTT_{90}	0.050	0.060
PTT_{80}	0.110	0.134
PTT_{70}	0.120	0.150
PTT_{30}	0.042	0.052
PTT_{20}	0.032	0.040
PTT_{10}	0.010	0.015

in which, R_i and ϕ_i denote the ith particle fraction radius and the ith volume fraction of dispersed phase, respectively. The interfacial tension can then be estimated by fitting the experimental data to the Palierne model. Using (α) as fitting parameter, the best fit gives the interfacial tension.

We calculated the interfacial tension based on the weighted relaxation spectrum ($\tau H_{(\tau)}$) with the relaxation time (τ) for PTT/PC blends. In order to get the weighted relaxation spectrum the following equations were used:

$$G'_{(\omega)} = \int_{-\infty}^{\infty} [(H_{(\tau)}\omega^2\tau^2)/(1 + \omega^2\tau^2)]\, d(\ln \tau) \quad (16)$$

$$G''_{(\omega)} = \int_{-\infty}^{\infty} [(H_{(\tau)}\omega\tau)/(1 + \omega^2\tau^2)]\, d(\ln \tau) \quad (17)$$

the relaxation spectrum can be determined using Tschoegle approximation[46] as given in the following equation:

$$H_{(\tau)} = G'\left\{\begin{bmatrix}(d(\log G')/d(\log \omega)) - \\ 0.5(d(\log G')/d(\log \omega))^2\end{bmatrix} - [(1/4.606)[d^2(\log G')/d(\log \omega)^2]]\right\}_{1/\omega=\tau/\sqrt{2}} \quad (18)$$

where ω is the frequency and τ is the relaxation time. It should be noted that for a neat polymer one will get one relaxation time where as for blends two relaxation times τ_1 and τ_2 corresponding to the component polymers. The difference in the values ($\tau_1 - \tau_2$) was used to calculate the interfacial tension between the polymers in the presence and absence of compatibilisers. The interfacial tension (α) was calculated using two methods:

(i) Palierne[13] (eq 19)

$$\alpha = \left[\frac{R_v\eta_m}{4\tau}\right]\left[\frac{(19K + 16)(2K + 3 - 2\phi(K - 1))}{(10(K + 1)) - (2\phi(5K + 2))}\right] \quad (19)$$

and (ii) Choi−Schowalter[16] (eq 20).

$$\alpha = \left[\frac{R_v\eta_m}{\tau}\right]\left[\frac{(19K + 16)(2K + 3)}{40(K + 1)}\right]\left[1 + \phi\left(\frac{5(19K + 16)}{4(K + 1)(2K + 3)}\right)\right] \quad (20)$$

where R_v is the volume average domain radius, η_m is the viscosity of the matrix, ϕ is the volume fraction of the dispersed phase, K is the viscosity ratio and is given as $K = \eta_d/\eta_m$ (η_d is the viscosity of the dispersed phase). Both these equations are similar to Taylor's equation.

The interfacial tension values of PTT/PC blends calculated from these equations are given in Table 1. In both methods, the blends show different interfacial tension values, even though the difference is small. It is very interesting to note that the blends show very low interfacial tension values, which means that there is considerable interaction between the blend components. This is because of the transesterification reaction that occurred under the reaction conditions, and the random copolyester formed as a result of the transesterification reaction between PTT and PC is the main factor for the change in miscibility. This random copolymer formed as a result of these exchange reactions acted as a compatibilizer in the initial stages of reactions. The expected chemical structures of the transesterification products are indicated in reaction Scheme 1.[47] It should be noted that when PC forms the dispersed phase the interfacial tension increases with increase in the PC content since the amount of

Scheme 1. Expected Chemical Structures of the Transesterification Products of PTT and PC in PTT/PC Blends

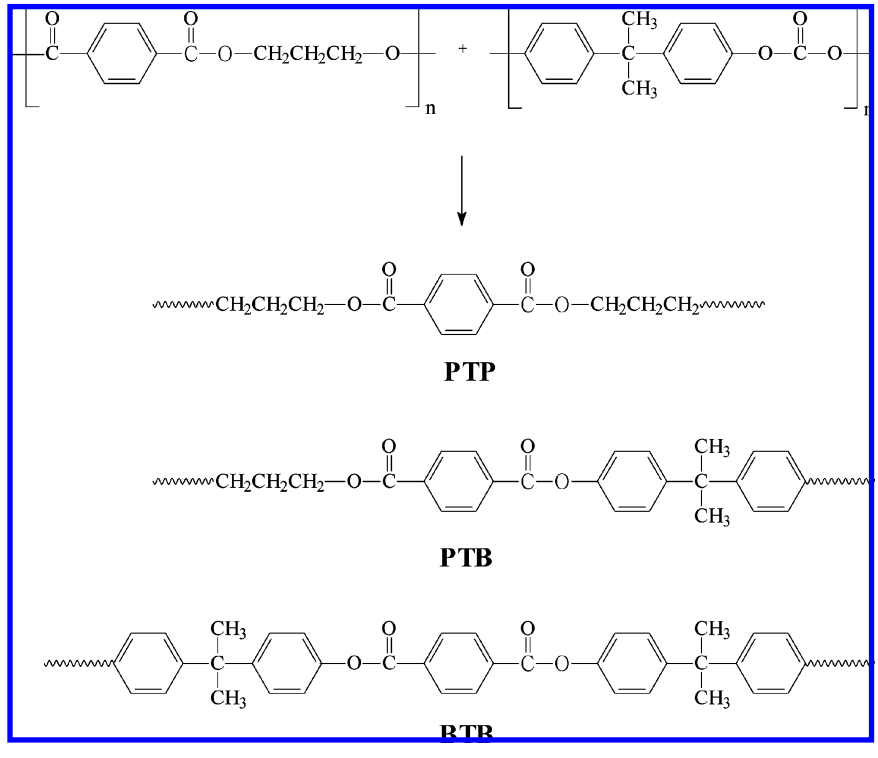

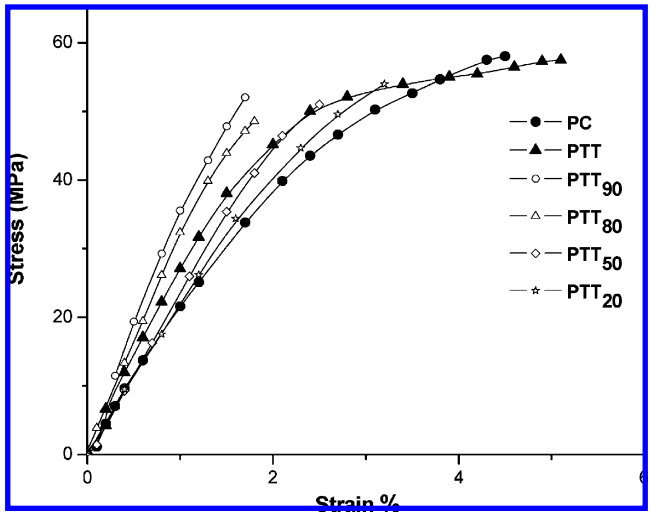

Figure 8. Stress−strain behavior of PTT/PC blends.

Table 2. Mechanical Properties of PTT/PC Blends

sample	ultimate tensile strength (MPa)	deformation at break (%)	Young's modulus (MPa)
PTT	59.5 ± 2.3	5.1 ± 0.24	2592 ± 39
PTT_{90}	52.1 ± 1.7	1.7 ± 0.04	2481 ± 41
PTT_{80}	48.1 ± 2.4	1.8 ± 0.03	2483 ± 29
PTT_{70}	46.2 ± 1.8	1.9 ± 0.04	2417 ± 33
PTT_{50}	48.4 ± 1.3	2.3 ± 0.03	2140 ± 46
PTT_{40}	51.3 ± 2.5	2.5 ± 0.03	2208 ± 30
PTT_{20}	57.3 ± 1.4	3.2 ± 0.04	2260 ± 44
PC	60.1 ± 1.2	4.5 ± 0.20	2189 ± 28

transreactions is more at high PTT content. But when PTT forms the dispersed phase, the interfacial tension decreases with increase in the PC content. The Palierne model gives lower interfacial tension values than the Choi−Schowalter model. However, for a polymer blend system, it is believed that irrespective of the blend composition, the interfacial tension should be the same. This slight difference between the α values arises from the parameter R_v, which is derived from the phase morphology. Note that since the blend is not a dilute system, the volume average particle size (R_v) contains contributions from interfacial tension as well as coalescence effect. Thus, the difference arises from the coalescence effect associated with R_v.

3.2. Mechanical Properties. For incompatible blends containing at least one semicrystalline component, the final tensile properties are determined by two competing factors: the increase in crystallinity due to the presence of a more crystalline component and the extent of compatibility between the two component polymers. The former is the property determining factor at low strain level, and the latter determines the properties at high strain level. The phase morphology and the interfacial adhesion between the component polymers also influence the mechanical properties of polymer blends. The stress−strain behavior of PTT/PC blends is demonstrated in Figure 8. From the stress−strain curves, we estimated maximum tensile strength (σ_m), elongation at break (E_b), and Young's modulus (E), and these tensile properties are summarized in Table 2. The results indicate that the addition of the PC phase decreases the tensile strength and modulus. A two-phase morphology with lack of adhesion between the component polymers leads to premature failure and thus to lower tensile strength.[48] The effect of the PC content on the ultimate tensile strength (σ_m) of PTT/PC blends is shown in Figure 9. Because of the poor adhesion between the components, the tensile strength shows negative

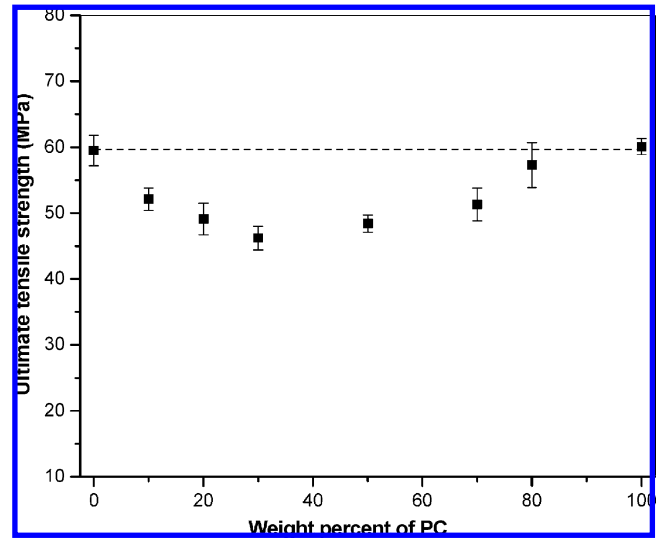

Figure 9. Effect of blend ratio on the ultimate tensile strength of PTT/PC blends.

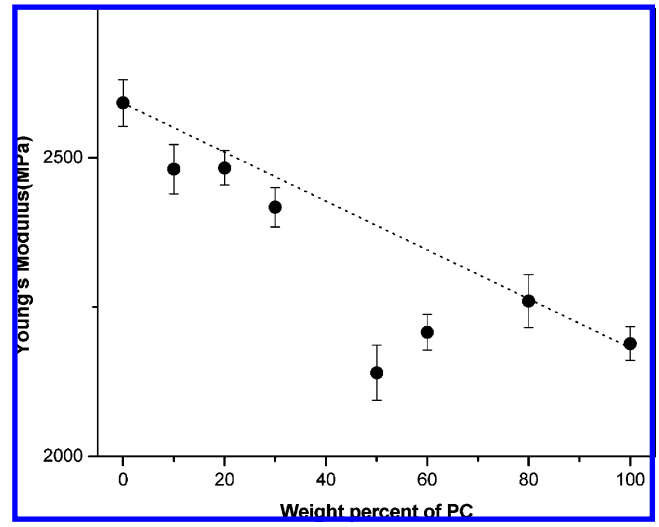

Figure 10. Effect of blend ratio on the Young's modulus of PTT/PC blends.

deviation from the additivity line. Addition of PC to PTT decreases the Young's modulus (E) of the blend system as indicated in Figure 10.

3.2.1. Theoretical Analysis of Mechanical Properties. In order to understand Young's modulus behavior, the applicability of various composite models such as parallel, series, Coran, and Takayanagi are examined.

The highest upper bound parallel model is given by the rule of mixtures as follows

$$E_u = \phi_1 E_1 + \phi_2 E_2 \tag{21}$$

This model is applicable to the materials in which the components are connected parallel to one another so that the applied stress lengthens each component to the same extent. In the lowest lower bound series model, the blend components are arranged in series (Reuss prediction) perpendicular to the direction of the applied force. The modulus prediction is given by the inverse rule of mixtures as:

$$\frac{1}{E_L} = \frac{\phi_1}{E_1} + \frac{\phi_2}{E_2} \tag{22}$$

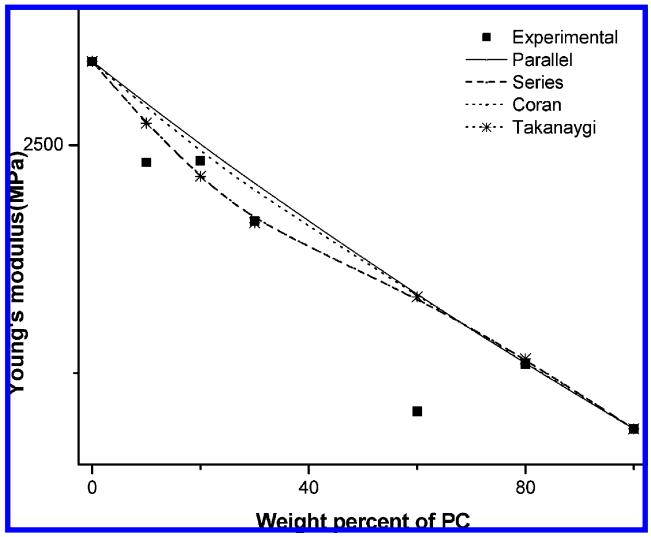

Figure 11. Plots of experimental and theoretical Young's moduli as a function of PC content.

In these models E_u is any mechanical property of the blend in the upper bound parallel model and E_L is the modulus of the blend in the series model. E_1 and E_2 are the mechanical properties of components 1 and 2, respectively; ϕ_1 and ϕ_2 are their corresponding volume fractions. For both these models, no morphology is required, but strain or stress can be continuous across the interface and Poisson's ratio is the same for both phases.

According to Coran's equation[49,50]

$$M = f(M_U - M_L) + M_L \tag{23}$$

where f can vary between zero and unity. The value of f is given by

$$f = V_H^{\,n}(nV_S + 1) \tag{24}$$

where n contains the aspects of phase morphology and V_H and V_S are the volume fractions of the hard phase and soft phase, respectively.

Takayanagi proposed a series−parallel model[51,52] in which, the concept of percolation is introduced. It is a phenomenological model consisting of mixture rule between two simple models involving connection in series (Reuss prediction) or in parallel (Voigt prediction) of the components. According to this model,

$$E = (1 - \lambda)E_1 + [(1 - \phi)/E_1 + (\phi/E_2)]^{-1} \tag{25}$$

E_1 is the property of the matrix phase, E_2 is the property of the dispersed phase, and ϕ is the volume fraction of the dispersed phase and is related to the degree of series−parallel coupling. The degree of parallel coupling of the model can be expressed by

$$\%\ \text{parallel} = [\phi(1 - \lambda)/(1 - \phi\lambda)] \times 100 \tag{26}$$

We have generated data according to these models, and these results are presented in Figure 11. It can be seen that all the theoretical models are near to each other especially when PTT forms the dispersed phase. The experimental data show some agreement with the series, Coran, and Takayanagi models except for 60 wt % PC. These models take into account the morphological aspects of the blend, and this may be the reason why the experimental value shows agreement with these models. This shows that there is a small interaction between the blend components under the experimental conditions. The reason for this is the small amount of transesterification reaction between PTT and PC under the reaction conditions, i.e. melt blending, compression molding, etc., but the effect is not much.

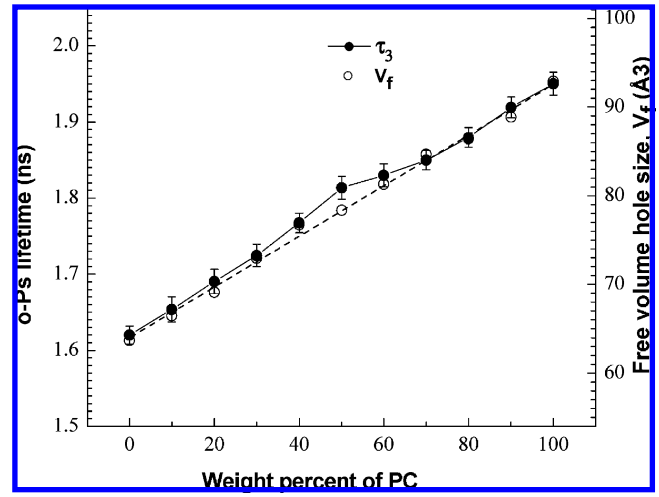

Figure 12. Effect of blend ratio on the *o*-Ps lifetime and free volume hole size of the PTT/PC blend.

3.3. Free Volume Measurements. The positron lifetime spectra from PALS measurements were resolved into three lifetime components τ_1, τ_2, and τ_3 with intensities I_1, I_2, and I_3, respectively. The shortest lifetime component τ_1 with intensity I_1 is attributed to *p*-positronium (*p*-Ps) and free positron annihilations. The intermediate lifetime component τ_2 with intensity I_2 is usually considered to be due to annihilation of positrons trapped at the defects present in the crystalline regions or trapped at the crystalline−amorphous interface. The longest-lived component τ_3 with intensity I_3 is due to pick-off annihilation of the *o*-Ps in the free-volume sites present mainly in the amorphous regions of the polymer matrix. The *o*-Ps lifetime τ_3 is related to the free-volume hole size by a simple relation developed by Nakanishi et al.[53] which is based on the quantum mechanical models of Tao[54] and Eldrup et al.[55] In this model, the positronium (Ps) atom is assumed to be localized in a spherical potential well having an infinite potential barrier of radius R_o with an electron layer in the region $R < r < R_o$. Accordingly, the relation between τ_3 and the radius R of the free volume hole or cavity is given by:

$$(\tau_3)^{-1} = 2\left[1 - \frac{R}{R_o} + \frac{1}{2\pi}\sin\left(\frac{2\pi R}{R_o}\right)\right] \tag{27}$$

where $R_o = R + \delta R$ and δR is an adjustable fitting parameter. The free-volume radius R was calculated from eq 27, and the average size of the free-volume holes V_f was evaluated as

$$V_f = (4/3)\pi R^3 \tag{28}$$

The relative fractional free volume or the free-volume content (F_{vr}) of the sample could then be estimated as

$$F_{vr} = V_f I_3 \tag{29}$$

To determine the free-volume parameters of the blends, we consider only the *o*-Ps lifetime τ_3 and its intensity I_3. The positron data of PTT/PC blends are shown in Figures 12 and 13. From these figures, it is clear that the average free volume size (V_f) and its intensity (I_3) increase slightly with increasing

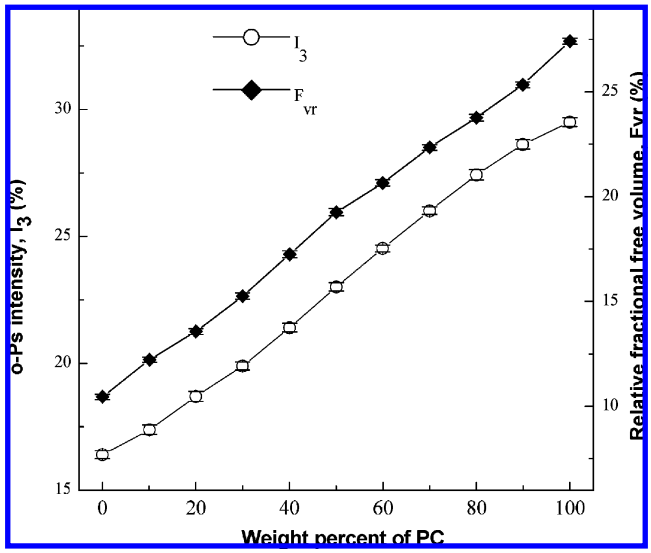

Figure 13. Effect of blend ratio on *o*-Ps intensity and relative fractional free volume in PTT/PC blends.

concentration of PC in the blend. This variation of the free-volume hole sizes of the blends was tested with the linear additivity rule and found to have a slight positive deviation from this rule.[56] The continuous but small increase in the free-volume hole size of the blend with increase of the PC content is possibly due to coalescence of the free volume of PC. Under normal blending conditions, the physical and chemical interactions across the phase boundaries of PTT and PC will be small. This leads to a weak interface. As a result, there is the possibility of void formation at the interface. But here, the samples used for PALS measurements are compression molded for 5 min after melt blending which is sufficient to induce transesterification reactions between the blend components. Therefore, the void formation becomes small, i.e. free volume values become small, and in PC rich blends the amount of transesterification reaction will be low, which means that an increase in free-volume size with increase in PC content is on the expected lines.

4. Conclusion

In the present investigation, the effect of blend ratio on the phase morphology, dynamic rheology, mechanical properties, and free volume of the PTT/PC blends was evaluated. Phase morphology analysis of the blends revealed that as the weight percent of PC in the PTT matrix increases the particle size increases and beyond a certain limit of composition (30 wt %) both PTT and PC form a cocontinuous phase structure. The phase inversion occurs at 60 wt % of PC where PC forms the matrix in which PTT is the dispersed phase. It is obvious that the less viscous component (PTT) forms smaller dispersed particles in the more viscous matrix (PC) due to comparatively restricted diffusion effects on coalescence of particles and increased shear stress resulting from the more viscous matrix phase. It was found that the complex viscosity of PTT/PC blends increased with increase in PC content. The melt viscosity values of the system have been compared with various theoretical models. The blends showed a positive−negative deviation of the measured viscosity from the additivity rule. This observation can be related to the change in phase structure with blend composition due to the transesterification reaction occurred under reaction conditions. The interfacial tension of the blends was determined using Palierne and Choi−Schowalter methods. The very low interfacial tension values of PTT/PC blends revealed that there is considerable interaction between the blend components due to the transesterification reactions. A random copolyester formed as a result of the transesterification reaction between PTT and PC, acted as a compatibilizer in the initial stages of reactions and is the main factor for the change in miscibility. The ultimate tensile strength and Young's modulus of uncompatibilized blends shows a negative deviation from the additivity line with increase in the PC component which demonstrated the incompatible nature of the blend components under normal conditions. The relatively small free-volume values indicate that there was a transesterification reaction which in turn decreases the free volume parameters. The relatively small increase in the free volume parameters of the PTT/PC blends with increase in the PC content showed the partial miscibility between the blend components suggesting interaction between the components at the interface.

Acknowledgment

The authors sincerely thank CSIR, New Delhi, India, for providing S.R.F. to one of the authors Mr. Indose Aravind. Authors are also thankful to Dr. Joseph V. Kurian and Sorona R&D, Bio-Based Materials, E. I. du Pont de Nemours and Company, Inc. Wilmington, Delaware 19880, for providing Sorona polymers for this study.

Literature Cited

(1) Utracki, L. A. *Polymer Blends Handbook*; Kluwer Academic Publishers: Netherlands, 2003.
(2) Favis, B. D. In *Polymer Blends*, Vol. 1, Paul, D. R., Bucknall, C. B., Eds.; Wiley Interscience: New York, 2000.
(3) Asadinezhad, A.; Yavari, A.; Jafari, S. H.; Khonakdar, H. A.; Boehme, F.; Haessler, R. *Polym. Bull.* **2005**, *54*, 205.
(4) Wu, S. *Polymer interfaces and adhesion*; Marcel Dekker Inc.: New York and Basel, 1982.
(5) Sanchez, I. C., Fitzpatrick, L. E., Eds. *Physics of polymer surfaces and interfaces*; Butterwort-Heinemann: Boston, 1992.
(6) Matsumoto, T.; Hori, N.; Takahashi, M. *Langmuir* **1996**, *12*, 5563.
(7) Utracki, L. A. *Commercial Polymer Blends*; Chapman & Hall: London, 1998.
(8) Araki, T.; Tran-Cong, Q.; Shibayama, M. *Structure and Properties of Multiphase Polymeric Materials*; Marcel Dekker Inc.: New York, 1998.
(9) Walheim, S.; Ramstein, M.; Steiner, U. *Langmuir* **1999**, *15*, 4828.
(10) Kim, H. J.; Seo, Y. *Langmuir* **2003**, *19*, 2696.
(11) Frankel, N. A.; Acrivos, A. *Chem. Eng. Sci.* **1967**, *22*, 847.
(12) Schowalter, W. R.; Chaffey, C. E.; Brenner, H. *J. Colloid Interface Sci.* **1968**, *26*, 152.
(13) Palierne, J. F. *Rheol. Acta* **1990**, *29*, 204.
(14) Loewenberg, M.; Hinch, E. J. *J. Fluid Mech.* **1996**, *321*, 395.
(15) Oldroyd, J. G. *Proc. R. Soc., London* **1953**, *A218*, 122.
(16) Choi, S. J.; Schowalter, W. R. *Phys. Fluids* **1975**, *18*, 420.
(17) Asthana, H.; Jayaraman, K. *Macromolecules* **1999**, *32*, 3412.
(18) Shi, D.; Ke, Z.; Yang, J.; Gao, Y.; Wu, J.; Yin, J. *Macromolecules* **2002**, *35*, 8005.
(19) Friedrich, C.; Gleinser, W.; Korat, E.; Maier, D.; Wees, J. *J. Rheol.* **1995**, *39*, 1411.
(20) Coran, A. Y.; Patel, R. *J. Appl. Polym. Sci.* **1976**, *20*, 3005.
(21) Sengers, W. G. F.; Sengupta, P.; Noordermeer, J. W. M.; Picken, S. J.; Gotsis, A. D. *Polymer* **2004**, *45*, 8881.
(22) Aravind, I.; Albert, P.; Ranganathaiah, C.; Kurian, J. V.; Thomas, S. *Polymer* **2004**, *454*925 14.
(23) Ravikumar, H. B.; Ranganathaiah, C. *Polym. Int.* **2005**, *54*, 1288.
(24) Ravikumar, H. B.; Ranganathaiah, C.; Kumaraswamy, G. N.; Thomas, S. *Polymer* **2005**, *46*, 2372.
(25) Chiu, F.-C.; Ting, M.-H. *Polym. Test.* **2007**, *26*, 338.
(26) Huang, D.-H.; Woo, E. M.; Lee, L.-T. *Colloid Polym. Sci.* **2006**, *284*, 843.
(27) Lee, L. T.; Woo, E. M. *Colloid Polym. Sci.* **2004**, *282*, 1308.
(28) Yavari, A.; Asadinezhad, A.; Jafari, S. H.; Khonakdar, H. A.; Bohme, F.; Hassler, R. *Eur. Polym. J.* **2005**, *41*, 2880.
(29) Woo, E. M.; Hou, S.-S.; Huang, D.-H.; Lee, L.-T. *Polymer* **2005**, *46*, 7425.

(30) Xue, M.-L.; Yu, Y.-L.; Chuah, H. H. *J. Macromol. Sci. Part B.* **2007**, *46*, 603.
(31) Chiu, F. C.; Lee, H. Y.; Wang, Y. H. *J. Appl. Polym. Sci.* **2008**, *107*, 3831.
(32) Kirkegaard, P.; Pedersen, N. J.; Eldrup, M. *Riso Nat. Lab. Reports, Denmark M* **1989**, 2740.
(33) Wu, S. *Polymer* **1987**, *28*, 1144.
(34) Lee, L. T.; Woo, E. M. *Colloid Polym. Sci.* **2004**, *282*, 1308.
(35) Utracki, L. A.; Kamal, M. R. *Polym. Eng. Sci.* **1982**, *22*, 96.
(36) Hashin, Z. *Second Order Effects in Elasticity, Plasticity, and Fluid Dynamics*; Reiner, M., Abir, S., Eds.; Macmillan: New York, 1964.
(37) Graebling, D.; Muller, R.; Palierne, J. P. *Macromolecules* **1993**, *26*, 320.
(38) Graebling, D.; Muller, R. *J. Rheol.* **1990**, *34*, 193.
(39) Bousmina, M.; Muller, R. *J. Rheol.* **1993**, *37*, 663.
(40) Carreau, P. J., Bousmina, M., Ajji, A., Ghiggin, K. P., Eds. *Progress in Pacific Science-3*; Springer-Verlag: New York, 1994.
(41) Lacroix, C.; Bousmina, M.; Carreau, P. J.; Favis, B. D.; Michel, A. *Polymer* **1996**, *37*, 2939.
(42) Vinckier, I.; Moldenaers, P.; Mewis, J. *J. Rheol.* **1996**, *40*, 613.
(43) Jansseune, T.; Mewis, J.; Moldenaers, P.; Minale, M.; Maffettone, P. L. *J. Non-Newtonian Fluid Mech.* **2000**, *93*, 153.
(44) Delaby, I.; Ernst, B.; Germain, Y.; Muller, R. *J. Rheol.* **1994**, *38*, 1705.
(45) Jacobs, U.; Fahrlander, M.; Winterhalter, J.; Friedrich, C. *J. Rheol.* **1999**, *43*, 1495.
(46) Tschoegle, N. W. *The Phenomenological Theory of Linear Viscoelastic Behaviour*; Springer: Berlin, 1989.
(47) Aravind, I.; Eichhorn, K.-J.; Komber, H.; Jehnichen, D.; Zafeiropoulos, N. E.; Ahn, K. H.; Grohens, Y.; Stamm, M.; Thomas, S. *J. Phys. Chem. B.* **2009**, *113*, 1569.
(48) Yang, H.; Lai, M.; Liu, W.; Sun, C.; Liu, J. *J. Appl. Polym. Sci.* **2002**, *85*, 2600.
(49) Coran, A. Y. *Handbook of Elastomers, New developments and Technology*; Bhowmick, A. K., Stephens, H. L., Eds.; Marcel Dekker: New York, 1988; p 249.
(50) Coran, A. Y. *Thermoplastic Elastomers*; Legge, N. R., Holden, G., Schroeder, H. E., Eds.; Hanser Publishers, Distributed by Macmillan Publishing Co; New York, 1987.
(51) Dickie, R. A. *J. Appl. Polym. Sci.* **1973**, *17*, 45.
(52) Miettiner, R. M. H.; Seppala, J. Y.; Ikkala, O. T.; Reima, I. T. *Polym. Eng. Sci.* **1994**, *34*, 395.
(53) Nakanishi, H., Wang, S. J., Jean. Y. C., Sharma, S. C., Eds. *Positron annihilation in fluids*; Singapore: World Scientific; 1988.
(54) Tao, S J. *J. Chem. Phys.* **1972**, *56*, 5499.
(55) Eldrup, M.; Lightbody, D.; Sherwood, N. *J. Chem. Phys.* **1981**, *63*, 51.
(56) Ravikumar, H. B.; Ranganathaiah, C.; Kumaraswamy, G. N.; Deepa Urs, M. V.; Jagannath, J. H.; Bawa, A. S.; Thomas, S. *J. Appl. Polym. Sci.* **2006**, *100*, 740.

Received for review May 8, 2009
Revised manuscript received July 14, 2009
Accepted July 16, 2009

IE9007503